Computational study of NLO responsive chromophores synthesized by green chemistry approach and second-order coefficients of graphitic oxide-chromophore hybrids

R. V. DODDAMANI, P. S. RACHIPUDI, D. D. ACHARI, M. Y. KARIDURAGANAVAR*
Department of Chemistry, Karnatak University, Dharwad-580 003, India

Using a green chemistry approach, different nonlinear optical (NLO) responsive chromophores were synthesized with indane-1,3-dione, imidazolidine-2,4-dione, pyrimidine-2,4,6(1H,3H,5H)-trione and 3-phenyl-2-isoxazolin-5-one as acceptors. The polarizability, hyperpolarizability, dipole moment and energy band gap between HOMO and LUMO of the optimized chromophores were calculated using DFT approach. With these chromophores, a series of graphene-based hybrid materials were prepared through covalent functionalization of chromophores onto the modified graphene oxide. The molecular structural characterizations of the chromophores and graphene-based hybrid materials were performed using FTIR, FT-Raman spectroscopy and ^{1}H NMR. Thermal behavior of the hybrid materials was investigated using TGA. The SHG coefficients (d_{33}) of the films were found to be in the range of 60.21 - 99.24 pm/V. From the results, the hybrid materials could be potential candidates for nonlinear optical devices.

1. Introduction

Nonlinear optics has fascinated the scientific community around the world owing to its applications in diverse fields, such as optical telecommunication, signal processing, data storage, image reconstruction, logic technologies, sensor protections and optical computing [1-3]. To address these applications, nonlinear optical (NLO) materials are playing vital role, and thus a large number of research groups have been actively involved in synthesis of NLO responsive organic molecules by employing various strategies. To enhance the NLO response in the organic molecules, donor–π–acceptor (D–π–A) is one of the most promising strategies [4]. The effectiveness of this strategy largely depends on the extent of π-conjugation and the strength of both donor and acceptor moieties [5,6]. In the recent literature, it is clearly indicated that the chromophores containing acceptors like hydantoin, barbituric acid have shown excellent second harmonic coefficient values. This is mainly because these two acceptors establish intermolecular hydrogen bonding between –NH and carbonyl groups [2,7]. Further, acceptors like 1,3-indanedione and 3-phenylisoxazol-5(4H)-one are proved to be excellent acceptors in view of their electron withdrawing ability, which is stronger than that of nitro or cyano- substituted acceptor moieties [8,9].

Recently, graphitic oxide (GO) has been used as potential π-conjugated extended bridges with large number of NLO responsive molecules [10]. Many polarizable π-electrons in the graphene could result in large second-order polarizability due to doubling frequency [11]. In addition, GO can be mass fabricated through the Hummer's method, which is simpler and more cost-effective than the carbon nanotube based nonlinear optical materials [12]. On the other hand, the two-dimensional (2D) graphene structure offers two dimensions for chemical functionalization either on the 2D π-conjugated network or on its edges. The oxygen containing groups present in the GO also make it partly hydrophilic. But these groups can be readily explored to functionalize the graphene sheets. Thus, resulting functionalization provides a means for the anchoring of nanoparticles and small molecules on the graphene sheets [13].

Over the past decade, a series of graphene-based hybrid materials, functionalized through covalent bonding or electrostatic adherence using porphyrin [14-16], phthalocyanines [17-19], oligothiophene [20], nanoparticles [21-23], carbazole [24], polymers [25,26] and metal complexes [27], have been reported. The hybrid materials are projected to qualify the improved NLO effect by the synergism of different mechanisms, namely reverse saturable absorption (RSA) or two-photon absorption (TPA) or nonlinear scattering (NLS) and photo induced electron or energy transfer [28]. Particularly, the graphene-based donor–acceptor materials have demonstrated excellent optical and photophysical properties. This is due to the charge-transfer phenomenon occurring mainly from the photo-excited organic chromophore units to the graphene layers [29]. Thus, graphene hybrids with good NLO properties become promising materials for applications in optical devices, such as optical limiters and optical shutters [30]. As a consequence, recent studies of

functionalized graphene showed that hybrid materials exhibit high nonlinear optical absorption coefficients in nanosecond and femtosecond timescales [31,32].

For instance, Liu et al. [33] synthesized oligothiophene functionalized graphene material and achieved excellent optical limiting properties. Zhu et al. [34] demonstrated the broadband optical limiting performance of graphene oxide–zinc phthalocyanines nanocomposite. Similarly, several research groups have studied the scope of graphene–porphyrin hybrids for NLO applications [35,36]. It is observed that metal free porphyrins with graphene oxide exhibited enhanced nonlinear absorption properties compared to graphene oxide with metal porphyrins in nanosecond time scale [37].

On the other hand, dipolar push–pull chromophores, which involve a donor and acceptor group, have been widely investigated for NLO and other optoelectronic properties [8,38,39]. Unfortunately, the synthesis of push-pull chromophores is a tedious process and expensive too. Even with expensive and specific catalysts, the reaction takes a longer time to have better yield. Further, the reaction is to be carried out in a dry organic solvent and that too under inert atmosphere; otherwise, the side products are formed. Consequently, the chromophores synthesized under this condition fail to get an acceptance from the optoelectronic industries for the development of NLO devices. To circumvent this, we have adopted a facile and an eco-friendly procedure to synthesize the push-pull type chromophores by reacting *p*-hydroxy benzaldehyde with different acceptors, such as hydantoin, barbituric acid, 1,3-indanedione and 3-phenylisoxazol-5(4H)-one. All the reactions were performed in water at ambient temperature without adding any catalyst and obtained excellent yields, in less than 10 minutes. Since water is the environment benign solvent used here, the burden of organic solvent disposal was completely eliminated. In this perspective, the synthetic protocol adopted here is a powerful green chemical technology procedure from both the economical and synthetic point of view [40].

Understanding the feasibility of GO for mass fabrication and its unique 2D structure, which offers functionality either on the π-conjugated network or on its edges, we have synthesized a series of covalently functionalized NLO responsive GO-chromophore hybrids. Prior to this, GO was functionalized with COCl groups in order to favor the reactivity between the GO and chromophore. The chemical structure of the chromophores, functionalization of GO and covalently attached GO-chromophore hybrid materials were systematically studied using different techniques. Thin films of the finally synthesized materials were prepared on indium-tin oxide (ITO) substrate. The nonlinear optical property and thermal stability were evaluated and discussed in correlation with the structures and their intrinsic properties. The dipole moment, polarizability and first order hyperpolarizability of the chromophores were also calculated theoretically using DFT approach and these data were used to signify the potentiality of the chromophores for NLO applications.

2. Experimental section

2.1. Materials and methods

Hydantoin, barbituric acid, 1,3-indanedione, 3-phenylisoxazol-5(4H)-one and p-hydroxybenzaldehyde were purchased from Sigma–Aldrich, Missouri, USA. Graphite flakes were procured from Alfa Aesar, Ward Hill, Massachusetts, USA. Monochloroacetic acid, potassium permanganate ($KMnO_4$), absolute ethanol, diethylacetate, chloroform, *N,N*-dimethylformamide (DMF), dimethylacetamide (DMAc), dimethyl sulphoxide (DMSO), N-methyl-2-pyrrolidone (NMP), diethyl ether, sodium nitrate ($NaNO_2$), sulphuric acid (H_2SO_4) and tetrahydrofuran (THF) were purchased from S. D. Fine Chemicals Ltd., Mumbai, India. THF and diethyl ether were dried and distilled before use. Deionized water was used throughout the work.

2.2. Instrumentation

The Fourier transform infrared (FT-IR) and Raman spectra were recorded on a Nicolet 6700 Thermo Fischer Scientific Spectrometer. The proton nuclear magnetic resonance (^{1}H NMR) spectra were recorded on a Bruker Avance 400 MHz spectrometer. The ultraviolet-visible (UV–Vis) spectra were measured using a JASCO V670 spectrophotometer. The fluorescence spectra were measured with Hitachi F7000, fluorescence spectrofluorometer. The thermograms of the samples were measured using Perkin–Elemer Diamond Q600 TGA/DTA thermogravimetric analyzer at a heating rate of 10 ºC/min in a nitrogen atmosphere. The results of elemental analyses for C, H and N were performed on a Perkin–Elemer PE 2400 CHN elemental analyzer. The melting points of samples were recorded with open capillary tubes on a Mel-Temp apparatus.

The 5 wt.% dispersions of the samples prepared in DMSO were filtered through a 0.20 µm Teflon membrane filter and the resulting solutions were used to prepare the thin films onto an indium–tin oxide (ITO) glass substrate using a spin coating technique at a rate of around 3000 - 3600 rpm. The films were dried for 5 h in a vacuum oven at 80 ºC to remove the residual solvents. The thickness (l_s) and refractive index (n) of the films, prepared by a spin coating technique on a silicon wafer substrate, were determined using M-2000-U, J. A. Woollam Ellipsometer with CompleteEASE software at a wavelength of 632.98 nm at 65º, 70º and 75º angles. The data were modeled with *β-spline absorbing film* single layer model and fitted for all the final hybrid materials.

The second harmonic measurements were performed utilizing the setup described in our previous papers [41,42]. A Mode-Locked Nd:YAG laser (Continuum Minilite-I, 6 ns pulse duration, 28 mJ maximum energy at 1064 nm, 10 Hz repetition rate) was used as a fundamental light source. The second harmonic signals generated by a *p*-polarized fundamental wavelength (1064 nm) were detected by a fast photodiode (FDS010, rise time 0.9 ns, Thorlabs) and an oscilloscope (Tektronix TDS 724D, Digital Phosphor

Oscilloscope) with a frequency of 500 MHz. While measuring the SHG, the sample was held at 45° angle to the incident laser beam to get a maximum SHG output. Potassium dideuterium phosphate (KDP) crystal as a standard was used as a reference sample.

2.3. Computational study

All the quantum calculations were performed using Gaussian 16 (Revision A.03) program package [44] by employing density functional theory (DFT) approach with the Becke-3-Lee-Yang-Parr (B3LYP) functional levels for the 6-311++(G)(d,p) basis set to predict the properties of the synthesized chromophores in a gas-phase with the optimized geometry.

2.4. Synthesis of chromophores

2.4.1. Synthesis of (5Z)-5-(4-hydroxybenzylidene) imidazolidine-2,4-dione a

While stirring, the imidazolidine-2,4-dione **1** (1.00 g, 1 mmol) was dissolved in water (15 ml), and to this *p*-hydroxybenzaldehyde **2** (1.22 g, 1 mmol) was added at once. After 6-8 min, the completion of the reaction was confirmed by TLC. The solid mass thus obtained was isolated by simple filtration and dried to yield white solid **a**. M.p.: 230-235 °C. Yield: 1.63 g (80%). FTIR (KBr, cm^{-1}): 3200-3090 (N-H, O-H), 1586, 1442 (C=C), 1673 (C=O). ^{1}H NMR (400 MHz, DMSO-d$_6$, δ): 6.45 (s, 1H; CH), 6.92 (d, 2H; Ar-H), 7.76 (d, 2H; Ar-H), 9.78 (s, 2H; NH), 10.55 (s, 1H; OH) ppm. C$_{10}$H$_8$N$_2$O$_3$ (204.18212): calcd.: C(58.82%), H(3.95%), N(13.72%) and O(23.51%); found: C(58.98%), H(3.59%) and N(12.92%).

2.4.2. Synthesis of 5-(4-hydroxybenzylidene)-2-thioxodihydropyrimidine-4,6 (1H, 5H)-dione b

The compound **b** was synthesized by following the similar procedure adopted for chromophore **a**. But in place of compound **1**, barbituric acid **3** (1.28 g, 1 mmol) was utilized to yield orange coloured chromophore **b**. M.p.: 200 °C (dec). Yield: 1.99 g (86%). FTIR (KBr, cm^{-1}): 3300-3050 (N-H, O-H), 1608, 1450 (C=C), 1721 (C=O). ^{1}H NMR (400 MHz, CDCl$_3$, δ): 6.45 (s, 1H; CH), 6.98 (d, 2H; Ar-H), 7.26 (s, 2H; NH), 7.81 (d, 2H; Ar-H), 9.86 (s, 1H; OH) ppm. C$_{11}$H$_8$N$_2$O$_4$ (232.19222): calcd.: C(56.90%), H(3.47%), N(12.06%) and O(27.56%); found: C(57.63%), H(3.07%) and N(11. 90%).

2.4.3. Synthesis of 2-(4-hydroxybenzylidene)-1H-indene-1,3(2H)-dione c

In a round bottom flask, 1,3-indanedione **4** (1.46 g, 1 mmol) was suspended in 5 ml of distilled water. Since indanedione is a light-sensitive compound, the flask was covered with an aluminum foil. To this, *p*-hydroxybenzaldehyde **2** (1.22 g, 1 mmol) was added at once and stirred for 5 min. The resulting yellow coloured solid was separated out. The completion of the reaction was

monitored by TLC. The product was isolated by filtration, purified by washing with excess quantity of 2% sodium carbonate solution and resulting compound was designated as chromophore **c**. M.p.: 250 °C. Yield: 2.08 g (83%). FTIR (KBr, cm^{-1}): 3240-3060. (N-H, O-H), 1573, 1461 (C=C), 1677 (C=O). ^{1}H NMR (400 MHz, DMSO-d$_6$, δ): 6.95 (d, 2H; Ar-H), 7.76 (s, 1H; CH), 7.92 (m, 4H; Ar-H), 8.53 (d, 2H; Ar-H), 10.84 (br, s, 1H; OH) ppm. C$_{16}$H$_{10}$O$_3$ (250.2488): calcd.: C(76.79%), H(4.03%) and O(19.18%); found: C(75.73%), H(4.37%) and O(20.29%).

2.4.4. Synthesis of (4Z)-4-(4-hydroxybenzylidene)-3-phenyl-1,2-oxazol-5(4H)-one d

The chromophore **d** was synthesized by following the similar procedure adopted for chromophore **a**. However, in place of compound **1**, the 3-phenylisoxazol-5(4H)-one **5** (1.61 g, 1 mmol) was utilized to yield orange coloured chromophore **d**. M.p.: >300 °C. Yield: 2.38 g (90%). FTIR (KBr, cm^{-1}): 3400-3330 (N-H, O-H), 1574, 1454 (C=C), 1726 (C=O). ^{1}H NMR (400 MHz, CDCl$_3$, δ): 6.94 (d, 2H; Ar-H), 7.51 (s, 1H; CH), 7.26 (d, 4H; Ar-H), 7.52-7.60 (d, 3H; Ar-H), 8.39 (br, s, 1H; OH) ppm. C$_{16}$H$_{11}$NO$_3$ (265.26344): calcd.: C(72.45%), H(4.18%), N(5.28%) and O(18.09%); found: C(71.99%), H(4.27%) and N(4.99%).

The reaction routes of chromophores **a-d** are presented in Scheme 1.

2.5. Synthesis of graphitic oxide from graphite

Graphitic oxide was prepared by modifying the Hummer and Offeman's method [45,46]. Briefly, 2 g of graphite, 2 g of NaNO$_3$ and 100 ml of H$_2$SO$_4$ were stirred together by keeping in an ice bath. To this, 6 g of KMnO$_4$ was slowly added portion-wise while stirring, and the rate of addition was controlled in order to maintain the temperature in between 15 and 20 °C. After addition, the temperature of the mixture was raised to 35 °C using water bath and stirred for about 1 h. The resulting thick paste was dispersed in 100 ml of de-ionized water and the temperature of the suspension was then raised to 98 °C. The suspension was further treated with 300 ml of deionized water and 20 ml of 30% H$_2$O$_2$ solution. The warm suspension solution was filtered and washed several times with deionized water until the pH of the filtrate become neutral and dried at 65 °C under vacuum.

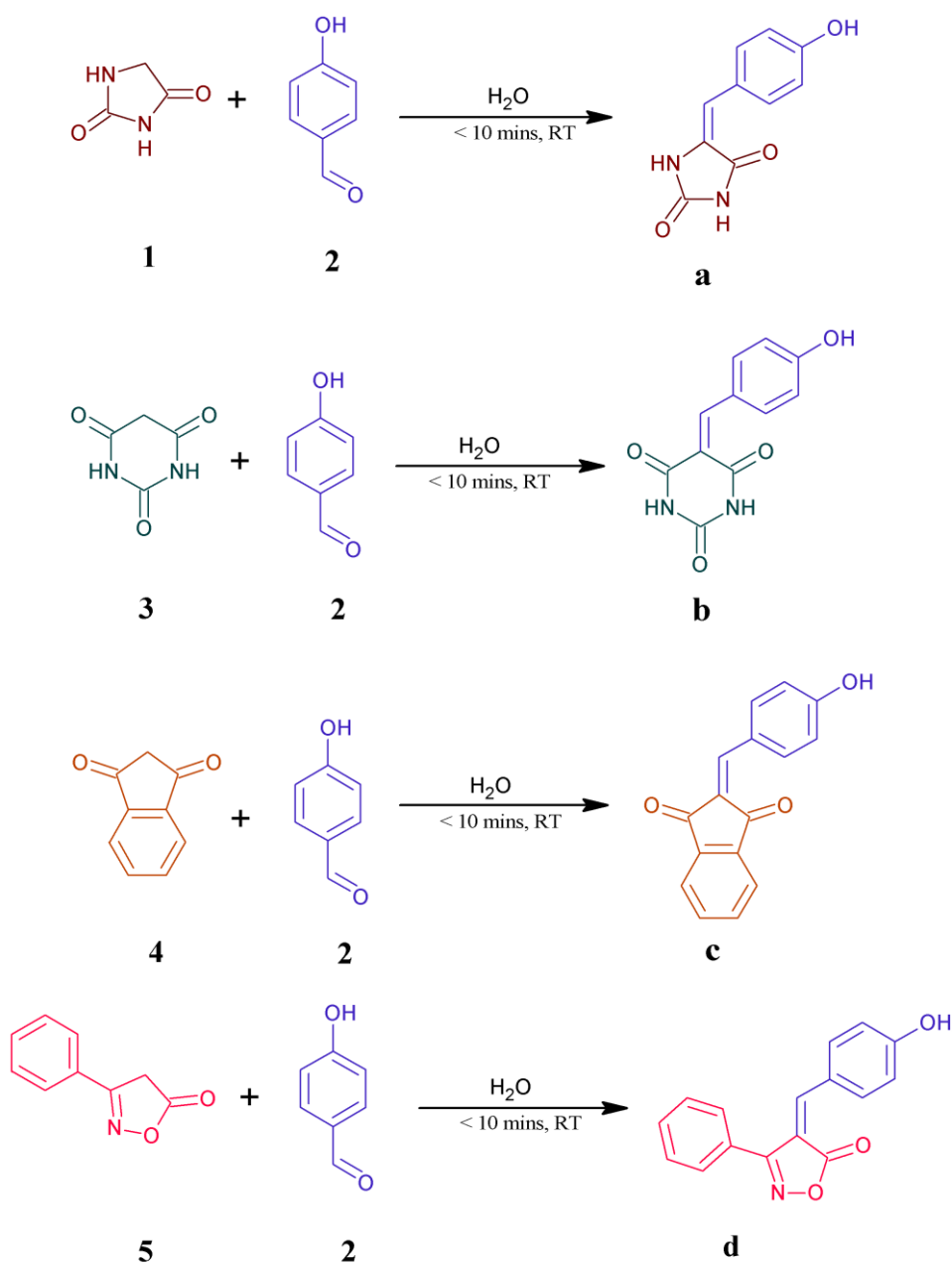The preparation of GO from the graphite is presented in Scheme 2.

2.5.1. Synthesis of GO-COOH

For the successful functionalization, the GO was dispersed in deionized water (1 mg ml^{-1}) and subjected to sonication for 3 h. It was then activated with 2.5 g of mono-chloroacetic acid under strongly basic condition (NaOH, 2.5 g) and sonicated for 3 h in order to promote –COOH groups on the surface of GO. The resulting functionalized (GO-COOH) solution was neutralized by adding excess quantity of deionized water and was purified by repeated rinsing and filtration.
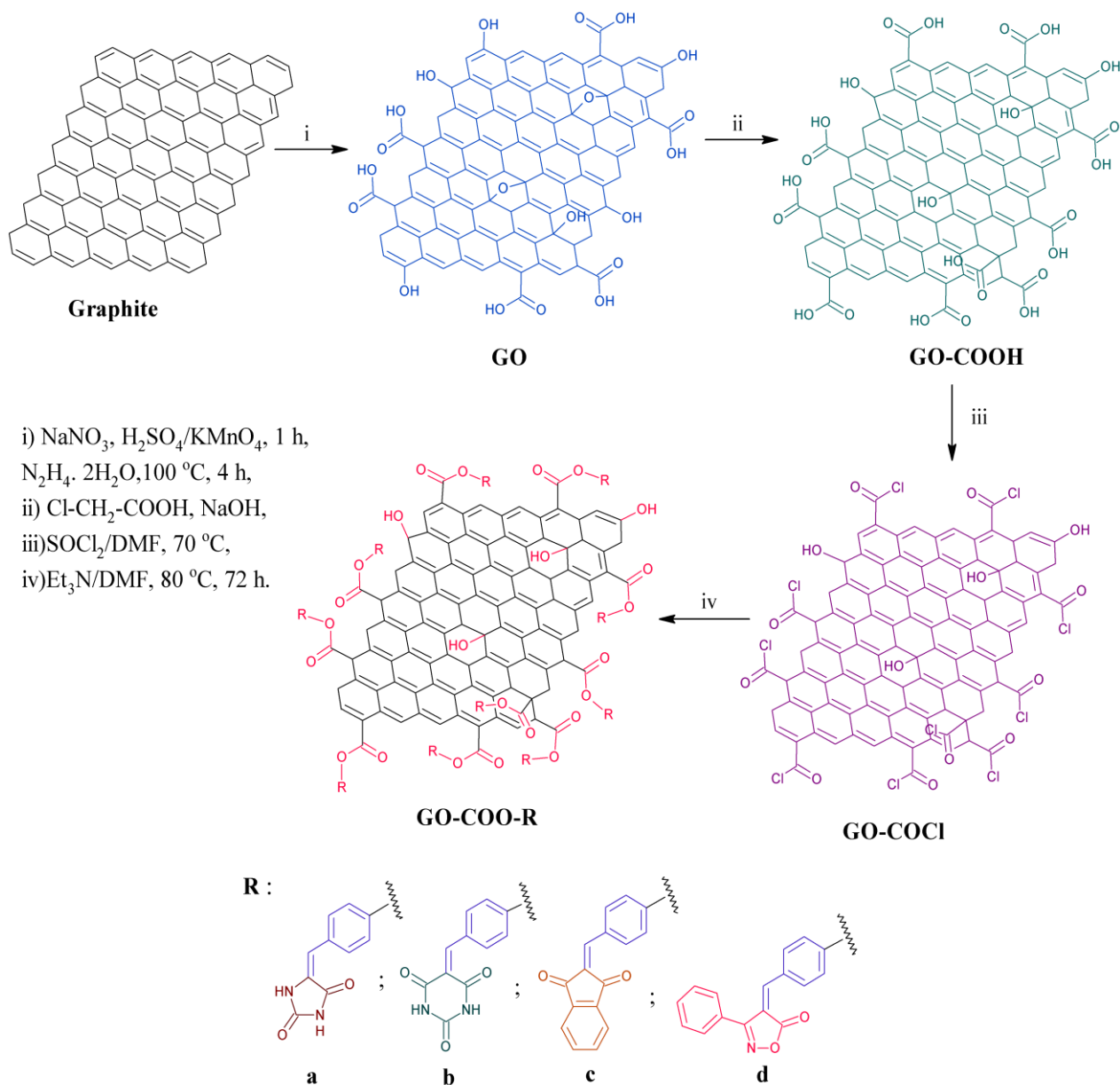
2.5.2. Synthesis of GO-COCl

The functionalized GO-COOH was reduced to GO-COCl with thionyl chloride in order to establish the covalent bonding between GO-COCl and chromophore. Briefly, the functionalized GO–COOH (0.5 g) was suspended in SOCl$_2$ (30 ml). To this, 5 ml of DMF was added and refluxed at 70 °C for 24 h under nitrogen atmosphere. The resulting solution was filtered and washed with anhydrous THF and dried under vacuum. The acylated graphene oxide (GO–COCl) was found to be 0.4953 g.

Scheme 1. Synthesis of chromophores a, b, c and d (color online)

i) NaNO$_3$, H$_2$SO$_4$/KMnO$_4$, 1 h,
N$_2$H$_4$. 2H$_2$O,100 °C, 4 h,
ii) Cl-CH$_2$-COOH, NaOH,
iii)SOCl$_2$/DMF, 70 °C,
iv)Et$_3$N/DMF, 80 °C, 72 h.

Scheme 2. Synthesis of GO-COO-R, graphene-chromophore hybrids (color online)

2.6. Synthesis of chromophores attached – graphene oxide hybrids (GO-COOR)

A mixture of GO–COCl (30 mg) and chromophore a (60 mg) was taken in a 50 ml capacity round bottom flask. To this, 3 ml of triethylamine and 15 ml of DMF were added and heated to 80 °C under a nitrogen atmosphere for 72 h to obtain a homogeneous black dispersion. The resulting dispersion was cooled to room temperature and poured into diethyl ether (300 ml). The precipitate thus formed was isolated by centrifugation at around 8000 rpm for 30 min. The supernatant that contained unreacted dissolved chromophore a was discarded. The isolated precipitate was again dispersed in 150 ml of diethyl ether and subjected to sonication for 30 min. It was then centrifuged at around 5000 rpm for 30 min and isolated the GO-COOR by discarding the supernatant. Finally, the precipitate was washed five times with CHCl$_3$ and dried. The TLC was used to check the supernatant layer to ensure no chromophore existed in the final washing. The same procedure was adopted for other three (b, c and d) chromophores.

The synthesis steps of functionalized GO and its graphene-chromophore hybrids (GO-COOR) are shown in Scheme 2.

3. Results and discussion

3.1. Synthesis and characterization of chromophores

The synthesis of chromophores a-d was performed at room temperature in water as a solvent. The reaction was completed in less than 10 min time without adding any

catalyst by following the Knoevenagel condensation reaction using p-hydroxybenzaldehyde 2 and selective heterocyclic compounds bearing active methylene groups, such as indane-1,3-dione, imidazolidine-2,4-dione, pyrimidine-2,4,6(1H,3H,5H)-trione and 3-phenyl-2-isoxazolin-5-one. The resulting chromophores were characterized by FTIR, 1H NMR, UV–vis and elemental analyses. The FTIR spectral data are consistent with the proposed structures of the chromophores as shown in Fig. 1. The 1H NMR spectrum of the chromophore c is presented in Fig. 2.
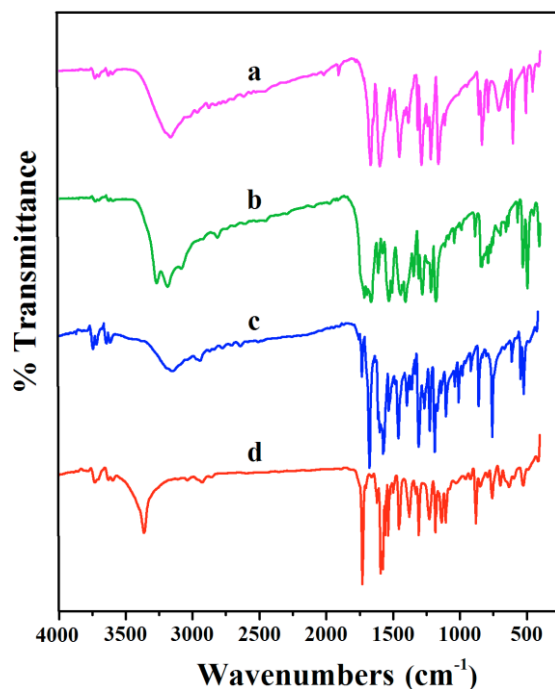
Fig. 1. The FTIR spectra of chromophores a-c (color online)
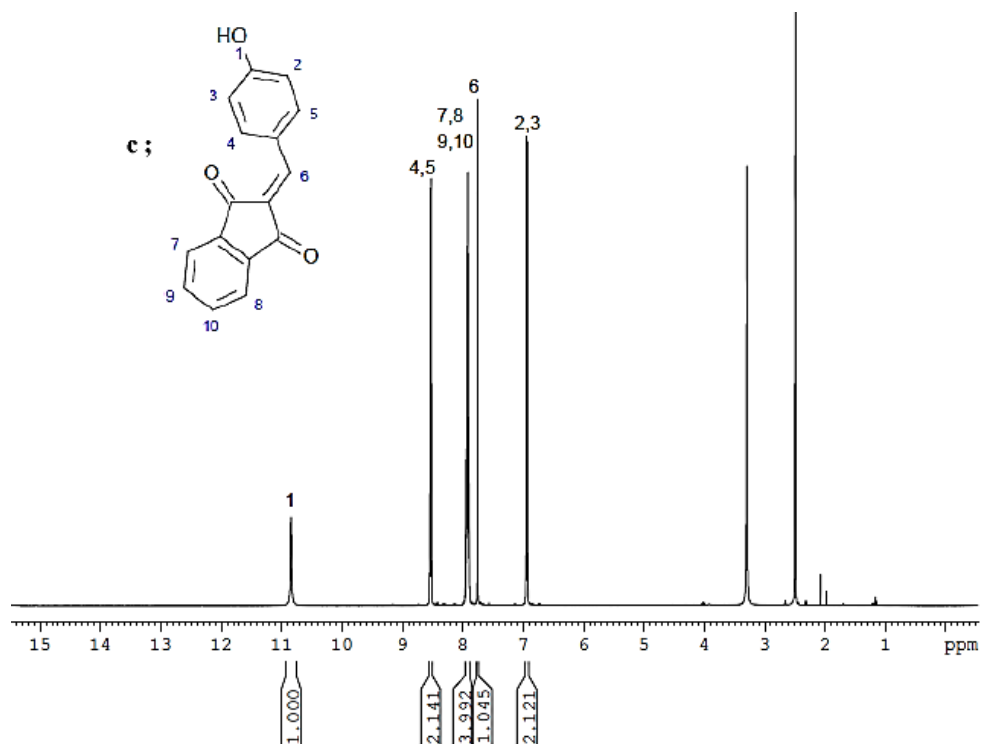
Fig. 2. The ^1H NMR spectrum of chromophore c

The spectrum showed two doublets at 6.95 and 8.53 ppm, and these were assigned to four aromatic protons. The multiplets resonated at 7.92 ppm were assigned to four aromatic protons. Similarly, the singlets appeared at 7.76 and 10.88 ppm were attributed to stilbene and hydroxyl protons, respectively. All these data including the elemental analyses confirmed the occurrence of reaction between p-hydroxy benzaldehyde and pyrimidine-2,4,6(1H,3H,5H)-trione.

The DMF solutions of chromophores a, b, c and d showed strong UV absorption maxima, respectively, at around 360, 455, 478 and 505 nm, respectively (Fig. 3). Similarly, we have recorded the fluorescence emissions spectra of all the chromophores a, b, c and d showed maxima emission, respectively, at 505, 575, 620 and 640 nm (Fig. 4). The high absorption and emission values (of especially chromophore d) is mainly because these acceptors (hydantoin, barbituric acid, 1,3-indanedione and 3-phenylisoxazol-5(4H)-one, respectively) establish intermolecular hydrogen bonding between –NH and carbonyl groups which perhaps give better NLO property.
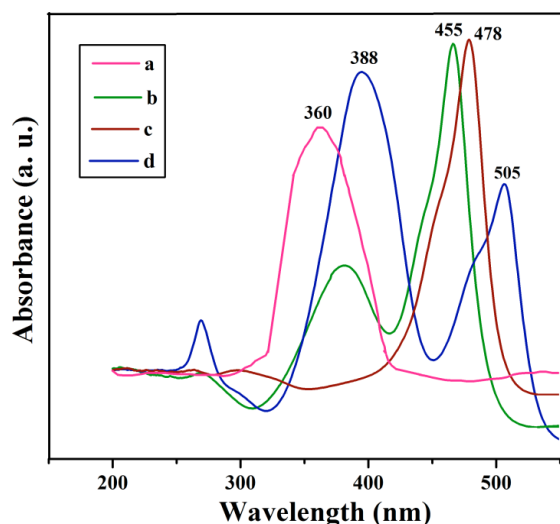

Fig. 3. UV-vis spectra of chromophores a, b, c and d (color online)

All these chromophores were soluble in organic solvents, such as ethanol, ethylacetate, chloroform, DMF, DMAc, DMSO and NMP. The synthesized chromophores are the push-pull type chromophores as shown in Scheme 1 with hydroxy group as the electron donor. The hydantoin, barbituric acid, 1,3-indanedione and 3-phenylisoxazol-5(4H)-one groups acted as the electron acceptors linked through a stilbene bridge.
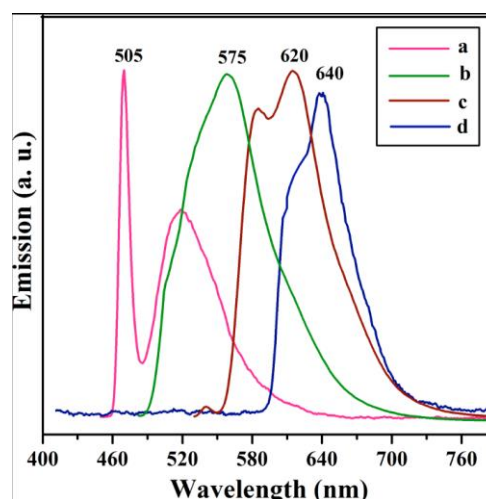

Fig. 4. Fluorescence spectra of chromophores a, b, c and d (color online)

3.2. NLO properties of chromophores: molecular modeling approach

The dipole moment (μ), the polarizability (α) and the first order hyperpolarizability (β) of the optimized geometries of the chromophores a, b, c and d were calculated using DFT/B3LYP/6-311++(G)(d,p). As commonly expressed in the literature, the isotropic (or average) polarizability is defined as [47, 48]:

$$\alpha = \frac{1}{3}(\alpha_{xx} + \alpha_{yy} + \alpha_{zz}) \qquad (1)$$

The first order hyperpolarizability of the chromophores **a**, **b**, **c** and **d** was calculated from Gaussian 16 output using eq. 2 with the x, y and z components:

$$\beta = \sqrt{(\beta_{xxx}+\beta_{yyx}+\beta_{zzx})^2+(\beta_{yyy}+\beta_{yxx}+\beta_{zzy})^2+(\beta_{zzz}+\beta_{zxx}+\beta_{zyy})^2} \qquad (2)$$

The calculated values of polarizability and the hyperpolarizability were converted from atomic units(au) into electrostatic units (esu), α: 1 a.u. = 0.148176 x 10^{-24} esu; β: 1 au = 0.863993 x 10^{-32} esu. The calculated values of α, β and μ of the chromophores were computed to be in the range of 24.7984 - 37.5184×10^{-24} esu, 1506.5116 - 3344.6923×10^{-32} esu and 2.2953 - 8.5335 Debye, respectively. All these data are presented in Table 1.

Table 1. The characteristic properties of chromophores calculated from the DFT approach

Chromophores	Dipole Moment μ (Debye)	Polarizability α (10^{24} esu)	Hyperpolarizability β (10^{32} esu)
a	2.2953	24.7984	1506.5116
b	2.8519	27.1784	2153.4414
c	4.9083	34.7034	2831.9188
d	8.5335	37.5184	3344.6923

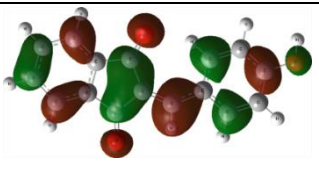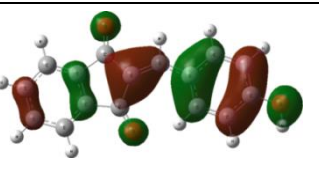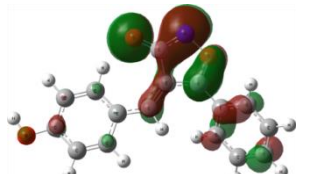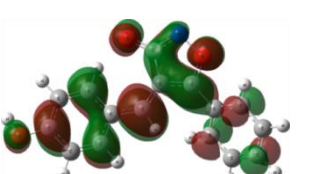The HOMO-LUMO of the optimized geometries of the chromophores are presented in Table 2. As can be seen from the structures, both HOMOs and LUMOs were delocalized over the entire molecule, and the electron density was equally distributed in two parts of the molecule. The surface energies of HOMO-LUMO and their energy band gap are included in the Table 2, which exhibited both molecular stability as well as electron delocalization are within the molecules. The energy band gap values ranged between 1.2254 - 1.9135 eV. From these, it is noticed that all the synthesized chromophores possessed small energy gap between the HOMO and LUMO; this signifies that the resulting molecules can be polarized easily. Among the chromophores, chromophore d showed the lowest energy gap, and this again signifies that chromophore d is the most polarizable molecule. Based on these data, it is concluded that the chromophores synthesized in the present study are proved to be the potential candidates for further NLO study.

3.3. Synthesis and characterization of GO and its functionalization

The FTIR spectra of GO and functionalized GO are presented in Fig. 5. The characteristic intense band was observed at around 3400 cm^{-1}, which corresponds to O–H stretching vibrations. The bands appeared at 1725 and 1025 cm^{-1} are respectively attributed C=O and C–O stretching vibrations of the carboxylic groups. The appearance of the peaks at around 2900 cm^{-1} was assigned to the aromatic stretching vibrations of C–H bonds. However, when GO-COOH was functionalized to GO-COCl, no significant change in the spectrum of GO-COCl was observed. *COCl.* This is expected, since the prominent groups are unchanged.

Table 2 The optimized structures of the chromophores, molecular orbital surfaces of HOMO and LUMO, their energies and band gap

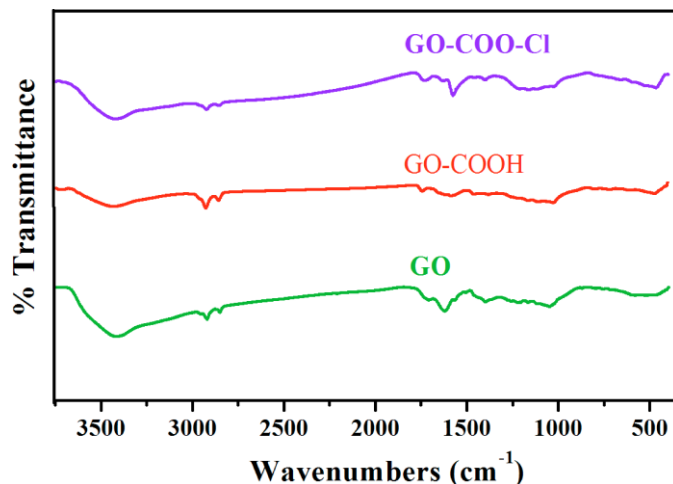|	Molecular orbital surfaces of HOMO	Molecular orbital surfaces of LUMO	HUMO (eV)	LUMO (eV)	Band gap (eV)
a			-3.4313	-1.5178	1.9135
b			-3.0233	-1.1832	1.8401
c			-3.2436	-1.4144	1.8292
d			-2.9716	-1.7462	1.2254
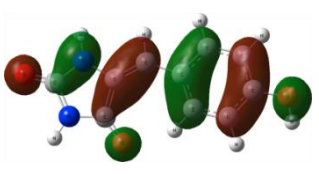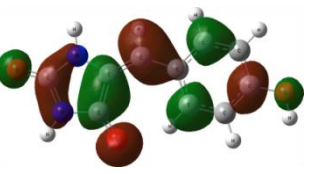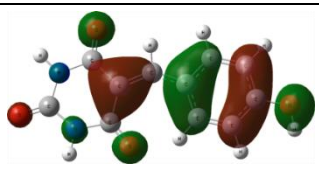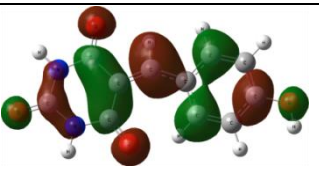
Fig. 5. The FTIR spectra of GO, GO-COOH and GO (color online)

After the functionalization of GO-COCl with the synthesized chromophores as shown in Fig. 6, the spectra of GO-COOR exhibited a prominent band at 1580 cm^{-1}, which corresponds to the C=C vibrations of the stilbene linkage established between the donor and acceptor molecules. The rest of the bands closely agree with the bands observed for chromophores. All these bands ascertain that the GO-COCl was successfully functionalized through covalent bonding between GO-COCl and the chromophores.
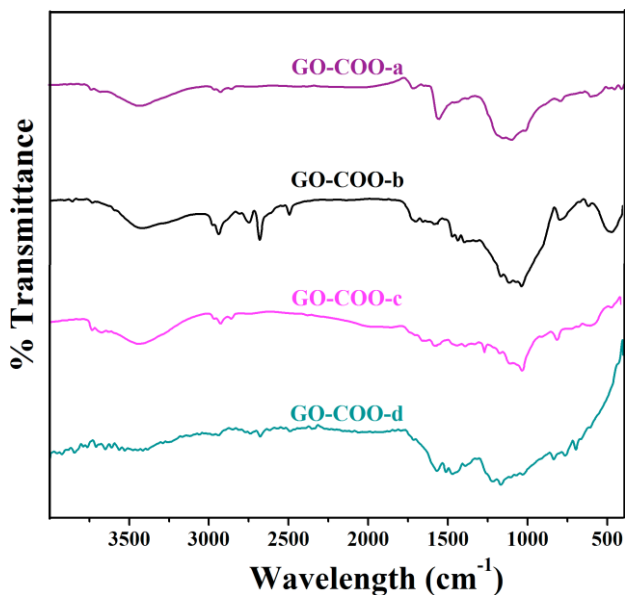

Fig. 6. The FTIR spectra of GO-COO-R hybrids (color online)

Upon oxidation, the graphite underwent a drastic change on the surface of its sp^2 planes. This was confirmed by recording the Raman modes of GO and its GO-COCl using FT-Raman spectrometer and the spectra are presented in Fig. 7.
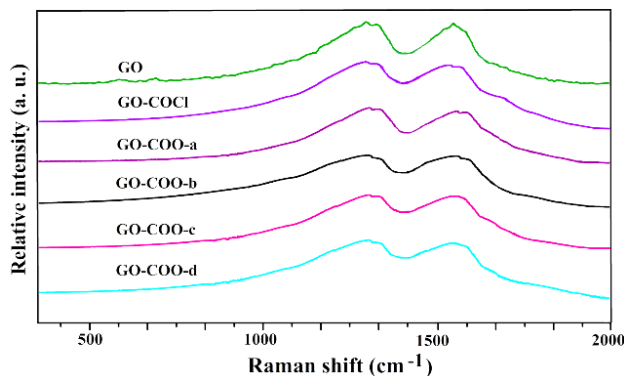

Fig. 7. The FT-Raman spectra of GO-COO-R hybrids (color online)

The spectrum of GO exhibited broad and weak Raman modes. This is expected due to the formation of edges and other defects in the graphene layers. The band appeared at 1335 cm^{-1} corresponds to D-band. Similarly, a broad band appeared at 1575 cm^{-1}, which corresponds to G-band. This is again due to disorder state of carbon in the graphene layers. A similar behaviour was also observed in the spectrum of GO-COCl. All these changes are attributed to significant decrease of sp^2 domains, which confirms the successful oxidation of graphite into GO and subsequently reduction of GO into GO-COCl. When chromophores attached to functionalized GO-COCl through covalent bonding, no significant change was noticed except the band position of D and G, which were marginally bands were shifted to 1334 and 1590 cm^{-1}, respectively. Apparently, this is due to slight change in the planes of the sp^2 domains. These evidences clearly support the functionalization of GO with the series of chromophores [36,46].

3.4. Thermal properties of GO-COO-R hybrids

The thermal stability of the GO-COO-R was analyzed by thermogravimetric analyses in the temperature range of ambient to 850 ℃ under N$_2$ atmosphere. From Fig. 8, it is observed that the weight loss of about 3 to 7 wt.% was noticed in all the thermograms upto 150 ℃. This is due to

weight loss of adsorbed moisture. Upto 200 ºC, none of the hybrid materials (GO-COO-R) underwent decomposition and this clearly suggests that all the synthesized hybrid materials demonstrated excellent thermal stability owing to the formation of ester bond between GO-COCl and the chromophores [45].
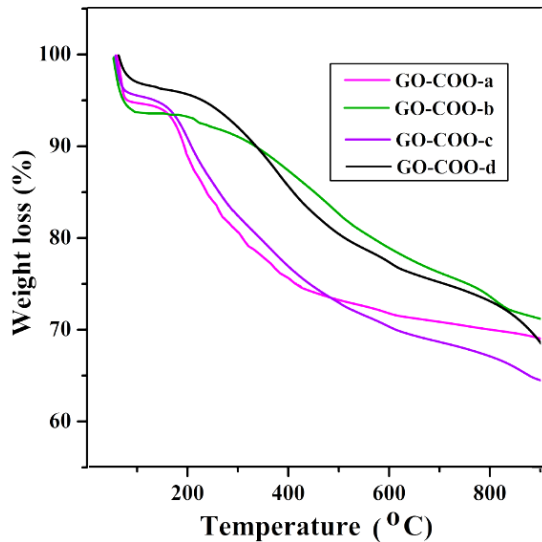

Fig. 8. The TGA thermograms of GO-COO-R hybrids (color online)

3.5. NLO properties of GO-COO-R hybrids

The nonlinear optical properties of the resulting GO-COO-R hybrids materials were examined using a Nd:YAG pulse laser. The SHG intensity of all the samples was measured at a fixed angle, $\theta = 45º$ and calculated the second-order NLO coefficients (d_{33}) using Eq. 3 [48-50]:

$$\frac{d_{33s}}{d_{36,k}} = \frac{\chi_s^{(2)}}{\chi_k^{(2)}} = \sqrt{\frac{I_s}{I_k}} \frac{l_{c,k}}{l_s} F \quad (3)$$

where $d_{36,k}$ is the d_{36} of KDP crystal, which is 0.40 pm/V; I_s and I_k are the SHG intensities of the samples and KDP crystal, respectively; $l_{c,k}$ is the coherence length of the KDP crystal (11.4 µm); l_s is the thickness of the sample film; and F is the correction factor, which is approximately equal to 1.2 when $l_{c,k} \gg l_s$. The calculated d_{33} values of the GO-COO-R and their film thicknessess are presented in Table 3.

Table 3. The physical and NLO properties of GO-COOR hybrids

GO-COOR hybrids	l_s[a] (µm)	n[b]	d_{33} (pm/V)
GO-COO-a	0.1000	1.5341	60.21
GO-COO-b	0.1127	1.3036	66.92
GO-COO-c	0.1000	1.2022	88.68
GO-COO-d	0.1000	1.4265	99.24

[a]Film thickness of hybrids measured using Ellipsometer
[b]Refractive index of hybrids measured using Ellipsomete

From the data, it is found that all the synthesized hybrid materials exhibited d_{33} values in the range of 60.21 - 99.24 pm/V. This suggests that the synthesized have demonstrated excellent second-order NLO coefficients. Among the series of developed materials, the chromophore d containing 3-phenyl-2-isoxazolin-5-one as an acceptor exhibited the highest d_{33} value. This might be due to the presence of additional phenyl ring on the isoxazolone moiety, which prevents the rotation of acceptor moiety across the stilbene linkage and thereby maintains the planarity in the chromophore structure. As a consequence, the flow of electrons becomes smooth from the donor group to acceptor moiety. Among the series of developed chromophores a-c, c exhibited relatively higher d_{33} value as compared to b and a. This is obviously due to fused phenyl ring, which again maintains planarity in the chromophore structure. As expected, chromophore b exhibited relatively higher d_{33} value as compared to a. This is because, b is more polar than that of a, and obviously the withdrawing ability of electrons in case of b was predominant. Thus, the acceptors' ability of chromophores is in the order d > c > b > a. The same trend was prevailed upon d_{33} values.

The second harmonic generation signals of all the GO-COO-R hybrid materials were monitored as a function of time at room temperature as well as at 110 ºC. However, only the data generated as a function of time at 110 ºC are presented in Fig. 9. All the samples were stable at room temperature and absolutely there was no decay in the intensity of the SHG signals. However, at 110 ºC in air, after an initial decay of ~5-10% of the original signal, more than 90% of the SHG signal remained stable even up to measured time of ~530 h for all the GO-COOR hybrid materials. This clearly supports that all the GO-COO-R hybrid materials favored better stability at the performed temperature and time.
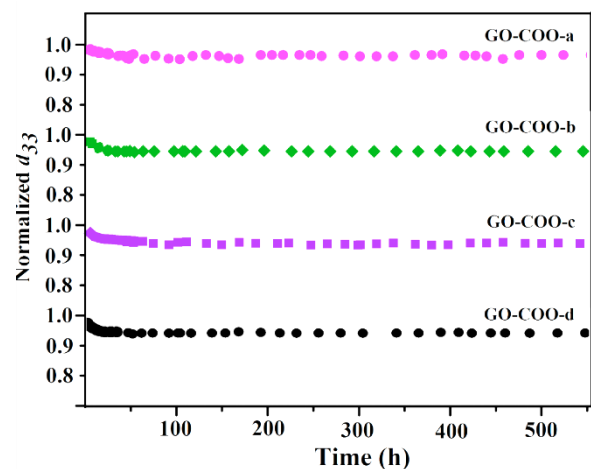

Fig. 9. The Temporal stability of SHG signals of GO-COO-R hybrids (color online)

In order to assess the temporal stability of the materials, SHG signals of all the resulting films were monitored as a function of temperature. For instance, the SHG signals of GO-COO-d recorded in Fig. 10. From the plot, it is observed that the SHG signals were stable up to 255 ºC, and

thereafter the SHG signals decreased rapidly, suggesting that the functionalized-GO containing chromophore d retained its thermal stability even up to 255 °C. Similar behaviour was also noticed for the remaining hybrid materials having chromophores a-c. Based on these thermal characteristics and optical nonlinearities, we strongly infer that the synthesized GO- functionalized hybrid materials are potential candidates for the applications of NLO devices.
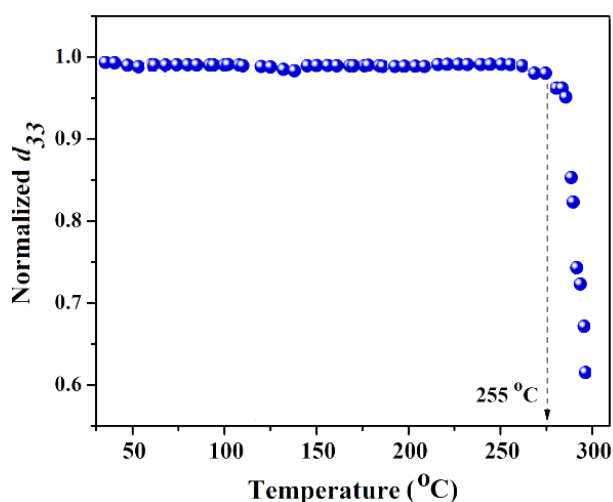

Fig. 10. The SHG signals of GO-COO-d hybrid (color online)

4. Conclusions

By employing a green chemistry approach, we have successfully synthesized the chromophores containing acceptors, such as hydantoin, barbituric acid, 1,3-indanedione and 3-phenyl-2-isoxazolin-5-one. The reactions were performed in water without using catalyst at room temperature. The time taken to complete the reaction was less than 10 min. Using these chromophores, a series of second-order NLO responsive GO-COOR hybrid materials was successfully prepared. All the analytical and spectral data were consistent with the proposed structures of the chromophores and the NLO responsive hybrid materials. The developed hybrid materials exhibited high thermal endurance owing to an establishment of ester bond between GO-COCl and the chromophores. Thus, the developed NLO responsive hybrids exhibited excellent thermal stability even at elevated temperatures. These hybrid materials exhibited relatively large d_{33} values, which ranged between 60.21 and 99.24 pm/V at 532 nm. Among the developed hybrid materials, containing chromophore d (GO-COO-d) demonstrated the highest d_{33} value of 99.24 pm/V with an excellent thermal stability (up to 250 °C). This was explained based on the additional phenyl ring, attached to the isoxazolone moiety. The chromophore d showed the lowest energy gap between HOMO and LUMO. This suggests that the chromophore d is the most predominant molecule for polarization. In view of the excellent nonlinearity and thermal stability, the developed

graphene based NLO materials could be of potential candidates for the construction of NLO devices.

References

[1] Y. Y. Melcamu, S. Wen, L. Yan, T. Zhang, Z. Su, Mol. Simulat. **39,** 214 (2003).
[2] M. Souto, J. Calbo, I. Ratera, E. Ortí, J. Veciana, Chem. Eur. J **23**, 11067 (2017).
[3] Ro Mu Jauhar, Paavai Era, V. Viswanathan, P. Vivek, G. Vinitha, D. Velmurugan, P. Murugakoothan, New J. Chem. **42**, 2439 (2018).
[4] M. Klikar, P. Le Poul, A. Ruzicka, O. Pytela, A. Barsella, K. D. Dorkenoo, F. R.-le Guen, F. Bures, S. Achelle, J. Org. Chem. **82**, 9435 (2017).
[5] B. J. Coe, S. P. Foxon, E. C. Harper, J. Raftery, R. Shaw, C. A. Swanson, I. Asselberghs, K. Clays, B. S. Brunschwig, A. G. Fitch, Inorg. Chem. **48**, 1370 (2009).
[6] J. S. Yang, K. L. Liau, C.Y. Li, M.Y. Chen, J. Am. Chem. Soc. **129**, 13183 (2007).
[7] N. Seferoglu, Y. Bayrak, E. Yalçın, Z. Seferoglu, J. Mol. Struct. **1149**, 510 (2017).
[8] K. Traskovskis, I. Mihailovs, A. Tokmakovs, A. Jurgis, V. Kokars, M. Rutkis, J. Mater. Chem. **22**, 11268 (2012).
[9] R. G. Tasaganva, M. Y. Kariduraganavar, R. R. Kamble, S. R. Inamdar, Synthetic Metals **161**, 1787 (2011).
[10] W. Jun, Y. Hernandez, M. Lotya, J. N. Coleman, W. J. Blau, Adv. Mater. **21**, 2430 (2009).
[11] D. R. Kanis, M. A. Ratner, T. J. Marks, Chem. Rev. **94**, 195 (1994).
[12] D. R. Dreyer, S. J. Park, C. W. Bielawski, S. R. Ruoff, Chem. Soc. Rev. **39**, 228 (2010).
[13] X. L. Zhang, Z. B. Liu, X. C. Li, Q. Ma, X. D. Chen, J. G. Tian, Y. F. Xu, Y. S. Chen, Opt. Express **21**, 7511 (2013).
[14] Z.-B. Liu, Y.-F. Xu, X.-Y. Zhang, X.-L.Zhang, Y.-S. Chen, J.-G. Tian, J. Phys. Chem. B **113**, 9681 (2009).
[15] Y. F. Xu, Z. B. Liu, X. L. Zhang, Y. Wang, J. G. Tian, Y. Huang, Y. F. Ma, X. Y. Zhang, Y. S. Chen, Adv. Mater. **21**, 1275 (2009).
[16] A. Wang, L. Long, W. Zhao, Y. Song, M. G. Humphrey, M.P. Cifuentes, X. Wu, Y. Fu, D. Zhang, X. Li, C. Zhang, Carbon **53**, 327 (2013).
[17] W. Song, C. He, Y. Dong, W. Zhang, Y. Gao, Y. Wu, Z. Chen, Phys. Chem. Chem. Phys. **17**, 7149 (2015).
[18] J. Zhu, Y. Li, Y. Chen, J. Wang, B. Zhang, J. Zhang,

W. J. Blau, Carbon **49**, 1900 (2011).

[19] W. Song, C. He, W. Zhang, Y. Gao, Y. Yang, Y. Wu, Z. Chen, X. Li, Y. Dong, Carbon **77**, 1020 (2014).

[20] Y. Liu, J. Zhou, X. Zhang, Z. Liu, X. Wan, J. Tian, T. Wang, Y. Chen, Carbon **47**, 3113 (2009).

[21] M. K. Kavitha, H. John, P. Gopinath, R. Philip, J. Mater. Chem. C **1**, 3669 (2013).

[22] M. Feng, R. Sun, H. Zhan, Y. Chen, Nanotechnology **21**, 075601(2010).

[23] T. He, W. Wei, L. Ma, R. Chen, S. Wu, H. Zhang, Y. Yang, J. Ma, L. Huang, G. G. Gurzadyan, H. Sun, Small **8**, 2163 (2012).

[24] T. Bai, C. Li, J. Sun, Y. Song, J. Wang, W. J. Blau, B. Zhang, Y. Chen, Chem. - Eur. J. **21**, 4622 (2015).

[25] P. Li, Y. Chen, J. Zhu, M. Feng, X. Zhuang, Y. Lin, H. Zhan, Chem. -Eur. J. **17**, 780 (2011).

[26] A. Midya, V. Mamidala, J. X. Yang, P. K. L. Ang, Z. Chen, W. Ji, K. P. Loh, Small **6**, 2292 (2010).

[27] J. Balapanuru, J. Yang, S. Xiao, Q. Bao, M. Jahan, L. Polavarapu, J. Wei, Q. Xu, K. P. Loh, Angew. Chem. Int. Ed. **49**, 6549 (2010).

[28] R. Liu, J. Hu, S. Zhu, J. Lu, H. Zhu, ACS Applied Materials and Interfaces **9**, 33029 (2017.

[29] A. Stergiou, G. Pagona, N. Tagmatarchis, Beilstein Journal of Nanotechnology **5**, 1580 (2014).

[30] Q. Ouyang, Z. Xu, Z. Lei, H. Dong, H. Yu, L. Qi, C. Li, Y. Chen, Carbon **67**, 214 (2014).

[31] M. Yue, J. H. Si, L. Yan, Y. Yu, X. Hou, Optical Materials Express **8**, 698 (2018).

[32] Z. B. Liu, X. L. Zhang, X. Q. Yan, Y. S. Chen, J. G. Tian, Chin. Sci. Bull. **57**, 2971 (2012).

[33] Y. Liu, J. Zhou, X. Zhang, Z. Liu, X. Wan, J. Tian, T. Wang, Y. Chen, Carbon **47**, 3113 (2009).

[34] J. Zhu, Y. Li, Y. Chen, J. Wang, B. Zhang, J. Zhang, W. J. Blau, Carbon **49**, 1900 (2011).

[35] K. Garg, R. Shanmugam, P. C. Ramamurthy, Carbon **122**, 307 (2017).

[36] M. Bala Murali Krishna, N. Venkatramaiah, R. Venkatesan, D. Narayana Rao, J. Mater. Chem. **22**, 3059 (2012).

[37] D. -J. Liaw, K. -L. Wang, Y. -C. Huang, K. -R. Lee, J. -Y. Lai, C. -S. Ha, Prog. Polym. Sci. **37**, 907 (2012).

[38] M. Souto, J. Calbo, I. Ratera, E. Orti, J. Veciana, Chem. Eur. J. **23**, 11067(2017).

[39] C. Li, M. Li, Y. Li, Y. Zhang, Z. Cai, Z. Shi, X. Wang, D. Zhang, Z. Cui, RSC Adv. **6**, 18178 (2016).

[40] R. V. Doddamani, R. G. Tasaganva, S. R. Inamdar, M. Y. Kariduraganavar, Polym. Adv. Technol. **29**, 1 (2018).

[41] M. L. Deb, P. J. Bhuyan, Tetrahedron Lett. **46**, 6453 (2005).

[42] R. G. Tasaganva, R. V. Doddamani, S. R. Inamdar, M. Y. Kariduraganavar, Optik **126**, 4991 (2015).

[43] S. M. Tambe, R. G. Tasaganva, S. R. Inamdar, M. Y. Kariduraganavar, J. Appl. Polym. Sci. **125**, 1049 (2012).

[44] M. J. Frisch, G. W. Trucks, H. B. Schlegel, G. E. Scuseria, M. A. Robb, J. R. Cheeseman, G. Scalmani, V. Barone, G. A. Petersson, H. Nakatsuji, X. Li, M. Caricato, A. V. Marenich, J. Bloino, B. G. Janesko, R. Gomperts, B. Mennucci, H. P. Hratchian, J. V. Ortiz, A. F. Izmaylov, J. L. Sonnenberg, D. Williams-Young, F. Ding, F. Lipparini, F. Egidi, J. Goings, B. Peng, A. Petrone, T. Henderson, D. Ranasinghe, V. G. Zakrzewski, J. Gao, N. Rega, G. Zheng, W. Liang, M. Hada, M. Ehara, K. Toyota, R. Fukuda, J. Hasegawa, M. Ishida, T. Nakajima, Y. Honda, O. Kitao, H. Nakai, T. Vreven, K. Throssell, J. A. Montgomery, Jr., J. E. Peralta, F. Ogliaro, M. J. Bearpark, J. J. Heyd, E.N. Brothers, K. N. Kudin, V. N. Staroverov, T. A. Keith, R. Kobayashi, J. Normand, K. Raghavachari, A. P. Rendell, J. C. Burant, S. S. Iyengar, J. Tomasi, M. Cossi, J. M. Millam, M. Klene, C. Adamo, R. Cammi, J. W. Ochterski, R. L. Martin, K. Morokuma, O. Farkas, J. B. Foresman, D. J. Fox, Gaussian, Inc., Wallingford CT, 2016.

[45] E. Jiang, H. Chunying, X. Xiangwu, D. Yongli, G. Yachen, C. Zhimin, W. Yiqun, S. Weina, Opt. Mater. **64**, 193 (2017).

[46] L. Tao, B. Zhou, G. Bai, Y. Wang, S.F. Yu, S.P. Lau, Y. H. Tsang, J. Yao, D. Xu, J. Phys. Chem. C **117**, 23108 (2013).

[47] S. Guidara, F. Habib, A. Younes, Spectrochem. Acta A **133**, 856 (2014).

[48] R. V. Doddamani, P. S. Rachipudi, N. A. Pattanashetti, M. Y. Kariduraganavar, New J. Chem. **43**, 15723 (2019).

[49] L. R. Dalton, C. Xu, A. W. Harper, R. Ghosn, B. Wu, Z. Liang, R. Montgomery, A. K. -Y. Jen, Nonlinear Opt. **10**, 383 (1995).

[50] R. V. Doddamani, P. S. Rachipudi, S. R. Inamdar, M. Y. Kariduraganavar, Polym. Eng. Sci. **9999**, 1 (2018).

_____

*Corresponding author: mahadevappayk@gmail.com